Grid Construction Strategies for Wall-Resolving Large Eddy Simulation and Estimates of the Resulting Number of Grid Points

Saleh Rezaeiravesh[1] and Mattias Liefvendahl[1,2]

[1]*Division of Scientific Computing, Uppsala University, Sweden*
[2]*Swedish Defence Research Agency (FOI), Sweden*

Abstract

Estimates of the total number of grid points required for wall-resolving large eddy simulation (WR-LES) of canonical wall-bounded turbulent flows, corresponding to different grid construction strategies, are derived. The common basis for all strategies is that the first off-wall grid spacing is of the order of the local viscous length scale. First, the estimate of the number of grid points for the block-nested grids, which are widely used in literature to calculate the computational cost of WR-LES, is reviewed in a general setting. Then, different functions, with appropriate controlling parameters, are introduced for distributing the grid points in the wall-normal direction. By using these functions along with assuming grid spacings in the streamwise and spanwise directions to be independent of the wall-normal coordinate, block-structured grids can be constructed, for which analytical expressions are derived to show the dependency of the total number of grid points to the flow Reynolds number. It is shown that under equivalent conditions, this class of grids demands more grid points than the block-nested ones. In particular, for a zero-pressure-gradient turbulent boundary layer at high Reynolds numbers, the increase in the number of grid points can be up to $\mathcal{O}(10^2)$, which relaxes to up to $\mathcal{O}(10)$ for fully-developed turbulent channel flow.

1 Introduction

In wall-bounded turbulent flows, the peaks of several important turbulent quantities such as production, dissipation, kinetic energy, and Reynolds stress are located in a thin layer near the wall, [4, 12, 14]. This justifies the necessity and importance of employing appropriate numerical methodologies for accurate simulation of the near-wall region. One of the key aspects to satisfy such a demand is to match the grid resolution requirements in the near-wall region with the appropriate length scale of the flow. In particular, in the framework of the current study, which is Wall-Resolving Large Eddy Simulation (WR-LES), the mentioned condition can be interpreted as enforcing the grid size and hence the filter width adjacent to the wall to be in the order of the flow viscous length scale, $\delta_\nu = \nu/u_\tau$, where ν denotes kinematic viscosity and the shear velocity is defined by $u_\tau = \sqrt{\tau_w/\rho}$ with τ_w and ρ representing wall shear stress and flow density, respectively.

To clarify this choice and also introduce the notations used throughout this report, consider a turbulent boundary layer (TBL) in the average sense, as schematically illustrated in Fig. 1. Based on a classical view, several subregions in the wall-normal direction can be considered including the inner layer, where the molecular shear dominates, and the outer layer, where the convective effects of the freestream play the most significant role, e.g. see [12, 20]. Corresponding to these two main regions, two different sets of characteristic velocity and length scales can be considered: length and velocity scales δ_ν and u_τ in the inner layer, in contrast to the boundary layer thickness δ, and the edge velocity U_e, in the outer layer. As a result of these scalings,

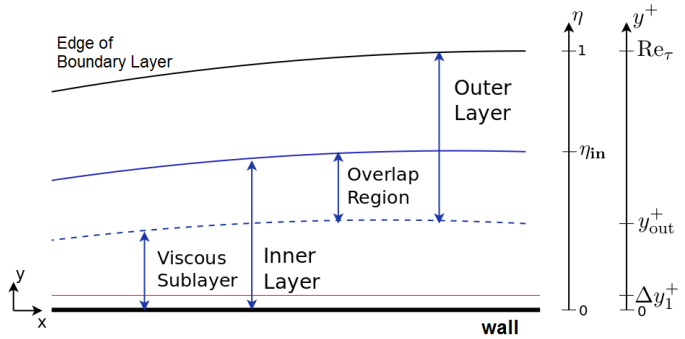

Figure 1: Schemetaic view of different regions in tutbulent boundary layer and their associated limits according to the inner and outer scalings.

the inner- and outer-scaled wall normal coordinates $y^+ = y/\delta_\nu$ and $\eta = y/\delta$, respectively, can be introduced that are related via $y^+ = \eta \mathrm{Re}_\tau$, where $\mathrm{Re}_\tau = \delta/\delta_\nu$ denotes one of the flow characteristic Reynolds numbers.

Once the distance of the first off-wall grid point is taken to be of the order of δ_ν, two more specifications of the grid remain to be specified. First, the distribution of the remaining points throughout the TBL, and second, specifying Δx and Δz, grid sizes in the streamwise and spanwise directions, respectively. Any particular choice made for these two specifications directly affects, $\mathrm{N_{wr}}$, the total number of grid points required for WR-LES. Deriving estimates for $\mathrm{N_{wr}}$ corresponding to different grid construction strategies for canonical wall-bounded turbulent flows constitutes the main body of this report.

In a widely-used strategy to derive estimates for $\mathrm{N_{wr}}$, [2, 3], layers of grid points are distributed within multiple blocks across the boundary layer in such a way that Δy remains constant in a block and it becomes larger as the block distance from the wall increases. In addition to this, Δx and Δz in each block are assumed to be proportional to the corresponding Δy. The estimated $\mathrm{N_{wr}}$ associated with this so-called block-nested grid, will be reviewed in Section 2. One of the main aims of this study is to derive similar estimates for the grids which look more like those being used in practical CFD simulations. In such grids, appropriate distributions of Δy in the wall-normal direction, satisfying the requirement of being of the order of δ_ν at the first off-wall grid point, are chosen. Moreover, contrary to the block-nested strategy, Δx and Δz are taken to be proportional to δ_ν. The general framework to derive estimates of $\mathrm{N_{wr}}$ for these grids, hereafter referred to as the block-structured grids, is derived in the beginning of Section 3, which is then followed by introducing three distribution functions for Δy constructed to reflect the appropriate scalings of the different regions of a TBL, in Section 3.1. In Section 3.2, the estimates made for the block-structured grids are derived and compared to those of the equivalent block-nested grids, for zero-pressure-gradient (ZPG) turbulent boundary layer. In the end, similar discussion is provided for fully-developed turbulent channel flow in Section 3.3.

2 Review of the Estimates for Block-Nested Grids

The main pioneer work for estimating the grid resolution requirements of WR-LES of turbulent boundary layers was performed by Chapman, [2]. In that derivation, one of the basic constraints was the fact that the grid resolution of the TBL is mostly driven by the viscous sublayer, $0 \leq y^+ \leq y^+_{\mathrm{out}}$, although it only constitutes a small part of the boundary layer.[1] The grids

[1] It must be noted that in the Chapman's analysis [2] and similarly in Choi and Moin [3], y^+_{out} was considered to be ≈ 100. According to the experimental results for a wide range of Re-numbers, Österlund et al. [11] proposed

covering the viscous sublayer were supposed to have the following specifications. The first off-wall grid point is located at $\Delta y_1^+ \approx 1-2$, which is chosen to be less than the Kolmogorov length scale (approximately 2 to 4 wall units), and Δy, the grid size in the wall-normal direction increases from Δy_1 to a specific fraction of the boundary layer thickness, i.e. δ/M, in the outer layer. In particular, parameter $\mathrm{M} > 0$ can be taken to be approximately equal to 25 consistent with the wall-modelled LES analysis [2], although it was later relaxed to 20 by Spalart et al. [18].

The block-nested strategy, schematically shown in Fig. 2, was employed by Chapman [2], in which the viscous sublayer is covered by several blocks each containing n_{y_s} points in the wall-normal direction. Furthermore, the ratio of Δx and Δz of each block to those of the previous one (located closer to the wall) is $r_x > 1$ and $r_z > 1$, respectively. All these constraints together result in the following number of grid points above a wall element with area $\mathrm{d}A = \mathrm{d}x\mathrm{d}z$ located at x, z,

$$\mathrm{dN_{wr}} = n_{y_s} \sum_n \left(\frac{1}{r_x r_z}\right)^n \frac{\mathrm{d}x\mathrm{d}z}{\Delta x_w \Delta z_w} \approx n_{y_s} \frac{r_x r_z}{(r_x r_z - 1)} \frac{\mathrm{d}x\mathrm{d}z}{\Delta x_w^+ \Delta z_w^+} \frac{1}{\delta_\nu^2}\,.$$

In this expression, Δx_w^+ and Δz_w^+ are the sizes of a grid located at the wall, in the streamwsie and spanwise directions, respectively, that are expressed in wall units. These two parameters can be chosen based on the requirements for resolving the turbulence structures existing in a part of the viscous sublayer where $y^+ \leq$ 5-15, e.g. see [12, 15, 14]. Through an analysis, Chapman [2] suggested to take $\Delta x_w^+ \approx 100$ and $\Delta z_w^+ \approx 20$ for resolving the streaks at small y^+. However in practice, different values of these parameters may be needed in order to produce accurate results, e.g. see [8, 9].

Although in the original work [2], an estimation for $\mathrm{N_{wr}}$ was obtained by using streamwise-averaged values for δ_ν in the above relation, Choi and Moin [3] derived an analytical expression by integrating the above relation over volume $(l_x - x_0) \times l_y \times l_z$, where, l_y specifies the thickness of the viscous wall region, x_0 denotes the initial non-turbulent length, and l_x and l_z are the domain lengths in the streamwsie and spanwise directions, respectively. To express $\delta_\nu = \nu/(U_e\sqrt{c_\mathrm{f}/2})$ in terms of Re_x-number, the power-law correlation $c_f = \alpha_f \mathrm{Re}_x^{-\beta_f}$, see Appendix A.1, can be used. Eventually, the total number of grid points constructed by the nested blocks, per aspect ratio (l_z/l_x), is estimated to be,

$$\frac{\mathrm{N_{wr}}}{(l_z/l_x)} \approx \frac{r_x r_z}{(r_x r_z - 1)} \frac{n_{y_s}}{\Delta x_w^+ \Delta z_w^+} \frac{\alpha_f}{2(1-\beta_f)} \mathrm{Re}_{l_x}^{(2-\beta_f)} \left[1 - \left(\frac{\mathrm{Re}_{x_0}}{\mathrm{Re}_{l_x}}\right)^{(1-\beta_f)}\right], \tag{1}$$

where, Re_{x_0} specifies the Re-number from which the boundary layer is considered to be fully turbulent. It is clear that for $\mathrm{Re}_{l_x} \gg \mathrm{Re}_{x_0}$, $\mathrm{N_{wr}}$ is proportional to $\mathrm{Re}_{l_x}^{(2-\beta_f)}$. In particular, Choi and Moin [3], estimated the asymptotic value of $\mathrm{N_{wr}}$ to be proportional to $\mathrm{Re}_{l_x}^{13/7}$, that is in contrast to the averaged value $\mathrm{N_{wr}} \sim \mathrm{Re}_{l_x}^{9/5}$ derived by Chapman [2]. It must be noted that despite slightly different approaches taken in the two mentioned studies, the main difference in the final estimations is due to the particular choices for β_f in the power-law correlation.

3 Estimates for Block-Structured Grids

As reviewed in the previous section, the estimations made for the grid number required for WR-LES are based on the assumption of having nested blocks. Although the computational

that y_{out}^+ can be ≈ 200 for high Re-number TBLs. This is in contrast to the classical view, e.g. see [12, 20], that assumes $y_{\mathrm{out}}^+ \approx 30-50$, which according to the mentioned analyses, [11], is considered to be associated with low-Re-number TBLs. For a review of the suggested values for y_{out}^+, see [10].

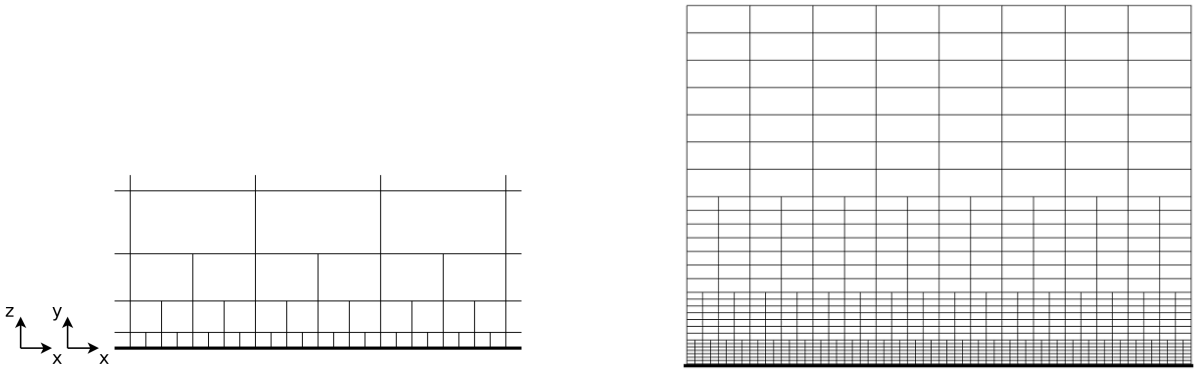

Figure 2: Schematic representation of (left) nested blocks, and (right) grid constructed by the nested blocks. For illustration purposes, vartiations of δ and Δy along the wall are neglected.

grid similar to what shown in Fig. 2 has been used in simulation of wall-bounded flows, e.g. [5], the structured grids can be considered to be more convenient for practical CFD simulations. This motivates deriving estimates of $\mathrm{N_{wr}}$ for the grids with Δy independently constructed in the wall-normal direction, and Δx and Δz considered to be proportional to the characteristic length of the inner part of the TBL.

To this end, it is assumed that a volume element $\mathrm{d}V = \mathrm{d}x\mathrm{d}y\mathrm{d}z$ within the TBL computational domain is covered by the grids of size $\Delta x \Delta y \Delta z$. This results in the following relation for the total number of grid points in domain $(l_x - x_0) \times \delta \times l_z$,

$$\mathrm{N_{wr}} = \int_{x_0}^{l_x} \int_{0}^{\delta(x)} \int_{0}^{l_z} \frac{\mathrm{d}x\mathrm{d}y\mathrm{d}z}{\Delta x \Delta y \Delta z} \,. \tag{2}$$

This formula is general, in the sense that it can be used for different forms of dependency of grid sizes Δx, Δy, and Δz, which lead to different grid construction strategies. As it was pointed out, to construct the block-structured grids, it is necessary to employ a function for distributing grid points in the wall-normal direction. Such a function is required to be controllable by proper parameters related to the flow characteristics and at the same time be applicable to practical simulations. Three of such distributions are introduced in next section which are then employed to evaluate (2).

3.1 Distribution Functions for Δy

The basic strategy to develop appropriate expressions for distributing Δy, is to locate the first off-wall point, given Re_τ and δ (these are in general, functions of x). For this purpose, $\Delta y_1^+ \approx 1 - 2$ can be chosen, for which the corresponding Δy is determined from,

$$\Delta y_1 = \frac{\Delta y_1^+}{\mathrm{Re}_\tau} \delta \,. \tag{3}$$

To discretize thickness δ above the wall, any of the following non-uniform distributions of Δy can be employed. It must be noted that without performing systematic simulations, no comments can be made on the performance of any of these distributions compared to the others. However, a set of example simulations of a particular case, based on these constructions is presented in Appendix A.2.

Compatible with Fig. 1, in the first distribution function, thickness δ is implicitly divided into

three layers with the associated grid spacing given by,[2]

$$\Delta\eta = \min\left[\max\left(\frac{\Delta y_1^+}{\mathrm{Re}_\tau}, \eta_{\mathrm{in}}\eta\right), \frac{1}{\mathrm{M}}\right] . \tag{4}$$

Note that parameter M must be chosen such that $(\eta_{\mathrm{in}}\mathrm{Re}_\tau) > \mathrm{M}$, to avoid a zero over-lap region in the mean velocity profile. As shown in Fig. 3, the grid points in the layer adjacent to the wall and also those located within $\eta_{\mathrm{in}} \leq \eta \leq 1$, have equal distances, while in the region between these two, Δy increases gradually with y.

Remark 1. It must be noted that according to the experimental data of ZPG-TBL and fully-developed channel flow, η_{in} has been found to be Re-dependent. In particular, for ZPG-TBL, Österlund et al. [11] reported η_{in} to be approximately 0.1125 and 0.15 for Re_θ less and greater than ≈ 6000, respectively, where $\mathrm{Re}_\theta = U_e\theta/\nu$ with θ denoting the momentum thickness. For channel flow, Zanoun et al. [21], found η_{in} to be approximately equal to 0.2 and 0.75 at low and high Re-numbers, respectively. It is also noticeable that, due to various types of uncertainties, different values for η_{in} have been suggested in literature, see [19, 10] and the references therein. Nonetheless, throughout this report, we ignore variation of η_{in} with Re-number for sake of simplicity.

In the second strategy, the grid points are distributed over two layers. In the first one, covering the inner part of the boundary layer, i.e. $0 \leq \eta \leq \eta_{\mathrm{in}}$, the sequence of grid spacings $\{\Delta y_j\}_{j=1}^{n_{y_l}}$ is constructed by,

$$\Delta y_j = \gamma^{j-1}\Delta y_1 \quad j = 1, 2, \cdots, n_{y_l} , \tag{5}$$

where, the constant stretching ratio between two successive grid spacings is defined by $\gamma = (\Delta y_j/\Delta y_{j-1}) > 1$. This ratio along with n_{y_l}, the number of points in the inner layer, must be determined, given Δy_1^+, Re_τ, and δ (and hence Δy_1, according to (3)). To this end, one of the required conditions is achieved by noticing that sequence (5), must satisfy $\Delta y_1^+ \sum_{j=1}^{n_{y_l}} \gamma^{j-1} = \eta_{\mathrm{in}}\mathrm{Re}_\tau$, that, in turn, is approximated by,

$$\Delta y_1^+ \frac{\gamma^{n_{y_l}}}{(\gamma - 1)} \approx \eta_{\mathrm{in}}\mathrm{Re}_\tau , \tag{6}$$

taking into account the properties of a geometric series with ratio γ^{-1}. Besides this, the other constraint is provided by choosing a certain value for the last increment in the grid size sequence. This relies on the assumption that in the outer part of the boundary layer, a set of equi-distance grid points can be used. This is in fact the main idea in estimating and constructing grids for the so-called wall-modelled LES, see [2, 3, 13, 7], where away from the near-wall region, number of grid points is proportional to δ. Therefore, $\Delta y_{n_{y_l}}$ is taken to be δ/M that can be equivalently expressed as $\Delta y_{n_{y_l}}^+ = \mathrm{Re}_\tau/\mathrm{M}$ in wall units. Combining the above constraints results in $\gamma = \eta_{\mathrm{in}}\mathrm{M}/(\eta_{\mathrm{in}}\mathrm{M} - 1)$, which can be plugged into (6) to determine n_{y_l}. As a result of this construction, the second layer which starts from the end of the inner layer and extends up to the edge of boundary layer is discretized by $n_{y_c} \approx \mathrm{M}(1-\eta_{\mathrm{in}})$ equally-spaced points with $\Delta y \approx \delta/\mathrm{M}$. It is recalled that in a more general manner, variability of η_{in} with Re-number may affect γ, n_{y_l}, and n_{y_c}. Eventually, the continuous form corresponding to the described distribution can be expressed by,

$$\Delta\eta = \begin{cases} \frac{\Delta y_1^+}{\mathrm{Re}_\tau} + \frac{\left(\gamma^{n_{y_l}-1}-1\right)}{\sum_{k=1}^{n_{y_l}}\gamma^{k-1}}\eta & , \eta \leq \eta_{in} \\ \mathrm{M}^{-1} & , \eta_{\mathrm{in}} \leq \eta \leq 1 \end{cases} . \tag{7}$$

The third type of grid construction in the wall-normal direction, can be achieved by simplifying the previous one. By construction, sequence $\Delta y_j = \gamma^{j-1}\Delta y_1$ starts from the wall and covers the

[2]This function is inspired by what mentioned in [12], p. 599, for channel flow. In the present work, the unspecified parameters in the original expression are chosen in connection with the characteristics of the canonical wall-bounded flows.

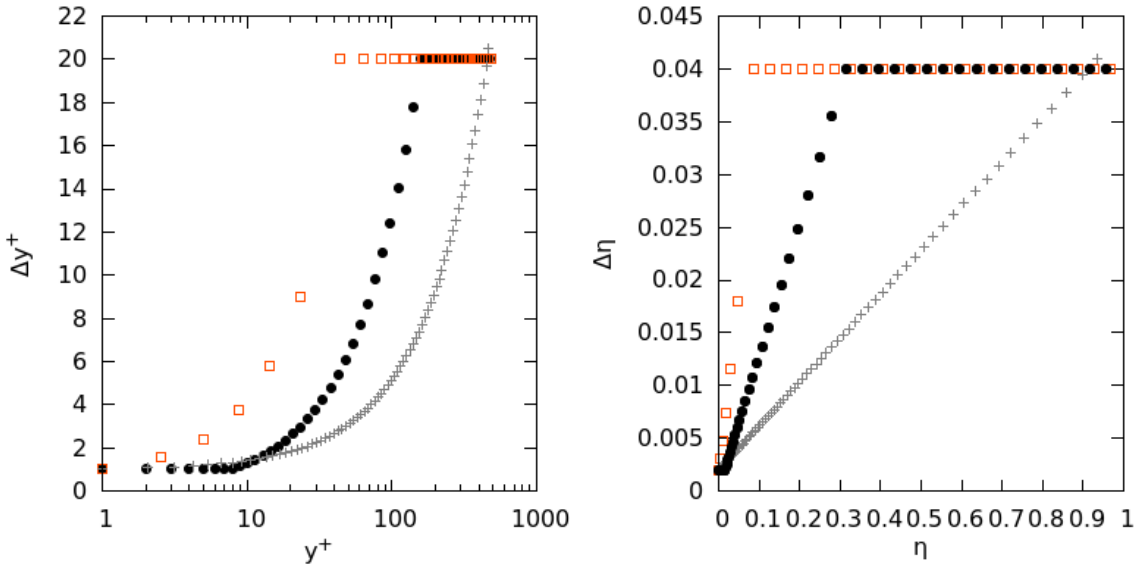

Figure 3: Distribution of grid points in the wall-normal direction, generated by different functions for $\mathrm{Re}_\tau = 500$, $\Delta y_1^+ = 1$, $\mathrm{M} = 25$, and $\eta_{\mathrm{in}} = 0.1125$.

whole thickness δ, without being constrained to be constant in the outer layer. However, the last increment is taken to be $\Delta y_{n_y} = \delta/\mathrm{M}$. Combination of these conditions leads to $\gamma = \mathrm{M}/(\mathrm{M}-1)$, that is Re-independent upon considering M to be fixed. However, the variation of Re-number affects the distribution through (3).

For a particular Re_τ, distributions of the grid points in the wall-normal direction generated by the above-described strategies are illustrated in Fig. 3. It is clear that for a particular Re-number, different constructions result in different number of grid points in the wall-normal direction. What is more interesting for us is to see how this dependency combined with the other influencing parameters will affect the estimates of N_{wr}.

3.2 Estimates of N_{wr} for ZPG-TBL

In this section, the focus is on deriving estimates of the number of grid points required for WR-LES of ZPG-TBL corresponding to each of the Δy distributions described in the previous section. Contrary to the block-nested counterpart, for constructing block-structured grid, Δx and Δz must be chosen independently for a given Δy distribution. However, it is still vital to relate them to an important characteristic of the boundary layer. In particular, the flow viscous length scale, δ_ν, is chosen for this purpose.

$$\begin{cases} \Delta x = a_x \delta_\nu \\ \Delta z = a_z \delta_\nu \end{cases}, \tag{8}$$

where a_x and a_z are two positive constant parameters. This setting simplifies the general expression (2) to,

$$\mathrm{N}_{\mathrm{wr}} = \frac{1}{a_x a_z} \int_{x_0}^{l_x} \int_0^{\delta(x)} \int_0^{l_z} \frac{1}{\delta_\nu^2} \frac{\mathrm{d}y}{\Delta y} \mathrm{d}z \mathrm{d}x \,. \tag{9}$$

It should be noted that due to the dependency of Δx and Δz on δ_ν, there will be enough resolution near the wall while the flow in the outer layer, where length scale $\delta \gg \delta_\nu$ governs the flow dynamics, is over-resolved in both x and z directions. This simply explains the computational efficiency of the block-nested grid compared to the block-structured one, under the

equal conditions. Before moving on further, it is noteworthy that δ_ν is not the only possible characteristic length based on which grid can be constructed for WR-LES. For instance, Addad et al. [1], used Taylor microscales to construct unstructured grids for wall-bounded turbulent flows.

To get a better understanding of the grids generated according to (8), we can focus on the developing ZPG-TBL over a flat plate. Since δ_ν increases in the streamwise direction, as given by (14) and shown in Fig. 4, for fixed a_x and a_z, grid sizes Δx and Δz become gradually larger along the wall as the boundary layer develops. However, this growth is not very significant even over a wide range of Re-numbers. Besides this, since the first off-wall grid spacing, Δy_1^+, is kept fixed in the whole domain, corresponding $\Delta\eta_1$ decreases, and $\Delta y_1 = \Delta y_1^+ \delta_\nu$ increases along the wall. One possible concern is that the number of grid points in the wall-normal direction required throughout the TBL, increases with Re-number. A remedy to this issue, can be using polyhedral cells in the framework of the finite-volume method.

Remark 2. It must be emphasized that the described method for grid construction differs from what is typically carried out in practice, which is based on obtaining grid sizes in accordance with the flow conditions at a specific location in the streamwise direction, and then using the same values in the whole domain. In such cases, if the value of δ_ν at the inlet is employed in (8), the flow simulation becomes over-resolved in x- and z-directions downstream. On the other hand, taking the number of grid points and spacings in the wall-normal direction in the whole domain to be equal to those at a spot with the highest Re-number, will lead to an excessive number of points over the wall at the upstream, without necessarily resolving the structures in the TBL.

The estimate of the number of grid points when distribution (4) is used in (9) is given by,

$$\begin{aligned}
\mathrm{N_{wr}} &= \frac{1}{a_x a_z}\int_{x_0}^{l_x}\int_0^{l_z}\frac{1}{\delta_\nu^2}\left[\int_0^{\frac{\Delta y_1^+}{\mathrm{Re}_\tau \eta_{\mathrm{in}}}} \mathrm{Re}_\tau \frac{\mathrm{d}\eta}{\Delta y_1^+} + \int_{\frac{\Delta y_1^+}{\mathrm{Re}_\tau \eta_{\mathrm{in}}}}^{\eta_{\mathrm{in}}} \frac{\mathrm{d}\eta}{\eta_{\mathrm{in}}\eta} + \int_{\eta_{\mathrm{in}}}^1 \mathrm{M}\mathrm{d}\eta\right]\mathrm{d}z\mathrm{d}x \\
&= \frac{1}{a_x a_z \eta_{\mathrm{in}}}\int_{x_0}^{l_x}\int_0^{l_z}\frac{1}{\delta_\nu^2}\left[1+\ln\left(\frac{\eta_{\mathrm{in}}^2\mathrm{Re}_\tau}{\Delta y_1^+}\right)+\eta_{\mathrm{in}}\mathrm{M}(1-\eta_{\mathrm{in}})\right]\mathrm{d}z\mathrm{d}x \\
&= \frac{1}{2a_x a_z \eta_{\mathrm{in}}}\left(\frac{U_e}{\nu}\right)^2\int_{x_0}^{l_x}\int_0^{l_z} c_{\mathrm{f}}\left[\chi_1+\ln \mathrm{Re}_\tau\right]\mathrm{d}z\mathrm{d}x\,,
\end{aligned}$$

where, $\chi_1 = \left[1+\ln(\eta_{\mathrm{in}}^2/\Delta y_1^+)+\eta_{\mathrm{in}}\mathrm{M}(1-\eta_{\mathrm{in}})\right]$. If one uses power law correlations $c_{\mathrm{f}} = \alpha_f \mathrm{Re}_x^{-\beta_f}$ and $\mathrm{Re}_\tau = \alpha_\tau \mathrm{Re}_x^{\beta_\tau}$, the above estimation for ZPG-TBL is more simplified as,

$$\begin{aligned}
\frac{\mathrm{N_{wr}}}{(l_z/l_x)} &= \frac{\alpha_f}{2a_x a_z(1-\beta_f)\eta_{\mathrm{in}}}\mathrm{Re}_{l_x}^{(2-\beta_f)}\left[\beta_\tau\left(f_1(\mathrm{Re}_{l_x})-\left(\frac{\mathrm{Re}_{x_0}}{\mathrm{Re}_{l_x}}\right)^{(1-\beta_f)} f_1(\mathrm{Re}_{x_0})\right)\right. \\
&+ \left.\chi_2\left(1-\left(\frac{\mathrm{Re}_{x_0}}{\mathrm{Re}_{l_x}}\right)^{(1-\beta_f)}\right)\right], \qquad (10)
\end{aligned}$$

where,

$$f_1(\mathrm{Re}_x) = \ln(\mathrm{Re}_x) - \tfrac{1}{(1-\beta_f)}\,,$$
$$\chi_2 = \chi_1 + \ln\alpha_\tau\,.$$

Similarly, by using distribution (7) in (9), the following estimate is achieved.

$$\begin{aligned}
\frac{\mathrm{N_{wr}}}{(l_z/l_x)} &= \frac{\alpha_f}{2a_x a_z(1-\beta_f)\chi_3}\mathrm{Re}_{l_x}^{(2-\beta_f)}\left[\left(f_2(\mathrm{Re}_{l_x})-\left(\frac{\mathrm{Re}_{x_0}}{\mathrm{Re}_{l_x}}\right)^{(1-\beta_f)} f_2(\mathrm{Re}_{x_0})\right)\right. \\
&+ \left.\mathrm{M}(1-\eta_{\mathrm{in}})\chi_3\left(1-\left(\frac{\mathrm{Re}_{x_0}}{\mathrm{Re}_{l_x}}\right)^{(1-\beta_f)}\right)\right], \qquad (11)
\end{aligned}$$

where,

$$\chi_3 = \left(\gamma^{n_{y_l}-1} - 1\right) / \sum_{k=1}^{n_{y_l}} \gamma^{k-1}\,,$$
$$f_2(\mathrm{Re}_x) = \beta_\tau \ln(\mathrm{Re}_x) + \chi_4\,,$$
$$\chi_4 = \ln\left(\alpha_\tau \chi_5\right) - \tfrac{\beta_\tau}{(1-\beta_f)}\,,$$
$$\chi_5 = \tfrac{\chi_3}{\Delta y_1^+}\eta_{\mathrm{in}}\,.$$

In derivation of this expression, approximation $\ln(1 + \chi_5 \mathrm{Re}_\tau) \approx \ln(\chi_5 \mathrm{Re}_\tau)$ which is valid for sufficiently high Re_τ, has been made to make analytical integration possible. In addition to this, dependence of n_{y_l} on Re_τ given by (6), was ignored for the same purpose.

Finally, the estimate corresponding to the third Δy distribution is derived to be,

$$\frac{\mathrm{N_{wr}}}{(l_z/l_x)} = \frac{\alpha_f}{2a_x a_z(1-\beta_f)\chi_6}\mathrm{Re}_{l_x}^{(2-\beta_f)}\left[f_3(\mathrm{Re}_{l_x}) - \left(\frac{\mathrm{Re}_{x_0}}{\mathrm{Re}_{l_x}}\right)^{(1-\beta_f)} f_3(\mathrm{Re}_{x_0})\right]\,, \tag{12}$$

where,

$$\chi_6 = (\gamma^{n-1} - 1)/\sum_{k=1}^{n} \gamma^{k-1}\,,$$
$$f_3(\mathrm{Re}_x) = \beta_\tau \ln(\mathrm{Re}_x) + \chi_7\,,$$
$$\chi_7 = \ln\left(\tfrac{a_\tau}{\Delta y_1^+}\chi_6\right) - \tfrac{\beta_\tau}{(1-\beta_f)}\,.$$

All estimations (10), (11), and (12) imply that, at sufficiently high Re-numbers, i.e. $\mathrm{Re}_{l_x} \gg \mathrm{Re}_{x_0}$, the $\mathrm{N_{wr}}$ of the block-structured grid is proportional to $\mathrm{Re}_{l_x}^{(2-\beta_f)} \ln(\mathrm{Re}_{l_x})$ rather than $\mathrm{Re}_{l_x}^{(2-\beta_f)}$ derived for the block-nested grid, see (1). At finite Re_{l_x}, the impact of the parameters on the estimates becomes more significant. In order to make a comparison between the $\mathrm{N_{wr}}$ estimated for the block-nested and block-structured grids, let us take Δx_w^+ and Δz_w^+ in construction of the block-nested grid to be fixed and known, and then relate a_x and a_z to them. For the particular choice $a_x = \Delta x_w^+$ and $a_z = \Delta z_w^+$, meaning that the near-wall resolution in the block-nested grid is used throughout the TBL in the block-structured strategy, variation of $\mathrm{N_{wr}}$ per aspect ratio (l_z/l_x), with Re-number is shown in Fig. 5. It can be seen that depending on the particular choice of the grid distribution in y-direction, the ratio of the $\mathrm{N_{wr}}$ of the block-structured grid to that of the block-nested one, may range from $\mathcal{O}(1)$ to $\mathcal{O}(10^2)$, with the largest ratio being associated with the case where distribution (4) is used for Δy. Although the advantage of any Δy-distribution employed here over the others is not proven, a general conclusion is that the block-nested strategy requires lower number of grid points than the block-structured one. As a result, it must be emphasized that the predicted computational power needed for WR-LES of TBLs at high Re-numbers, as made for instance in [17], can still be considered optimistic bringing into account that not all the CFD solvers are capable of handling the block-nested grids.

3.3 Estimates of $\mathrm{N_{wr}}$ for Fully-Developed Channel Flow

Similar to ZPG-TBL, grid estimates can be derived for WR-LES of fully-developed turbulent channel flow, for which length scale δ is constant, taken to be the channel half-width. Moreover, for this flow the lower bound x_0 in the integral becomes zero and the target Re_τ (the value to which the result of the numerical simulation supposedly converges) is taken to be fixed. These together, lead to significant simplifications in integral (9), reducing it to,

$$\mathrm{N_{wr}} = \frac{1}{a_x a_z}\left(\frac{l_x}{\delta}\right)\left(\frac{l_z}{\delta}\right)\mathrm{Re}_\tau^2 \int_0^\delta \frac{\mathrm{d}y}{\Delta y}\,. \tag{13}$$

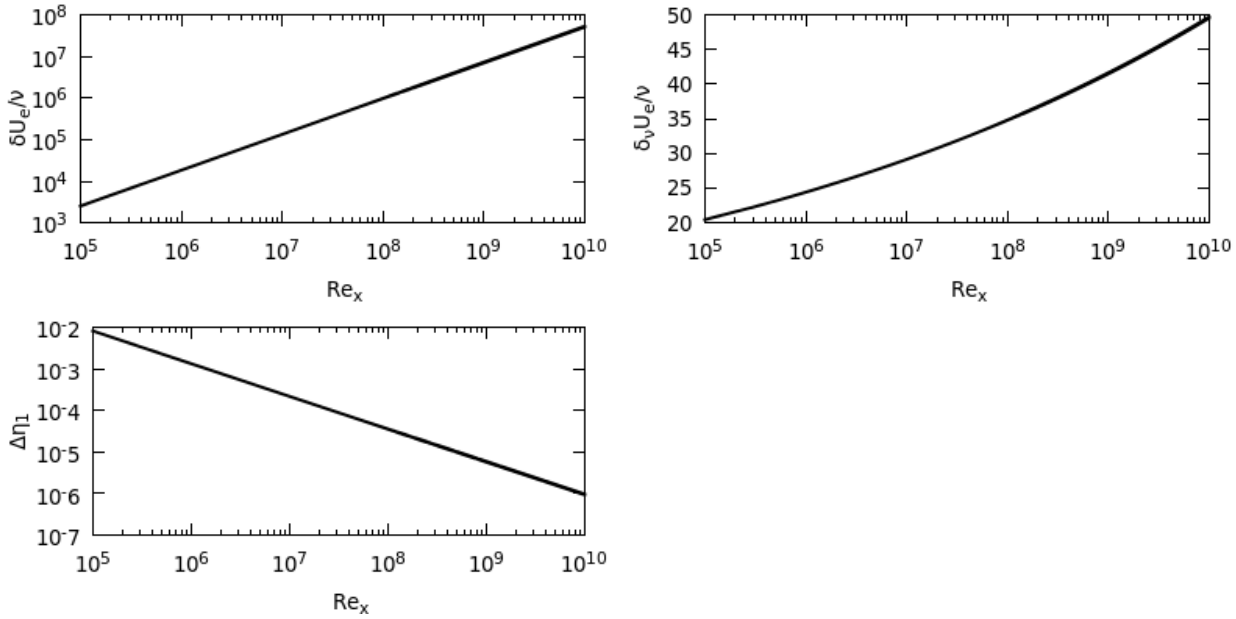

Figure 4: Variation of $\delta_\nu \frac{U_e}{\nu}$, $\delta \frac{U_e}{\nu}$, and $\Delta\eta_1$ (corresponding to $\Delta y_1^+ = 1$) with Re_x for ZPG-TBL, plotted by the power-law correlations given in Appendix A.1.

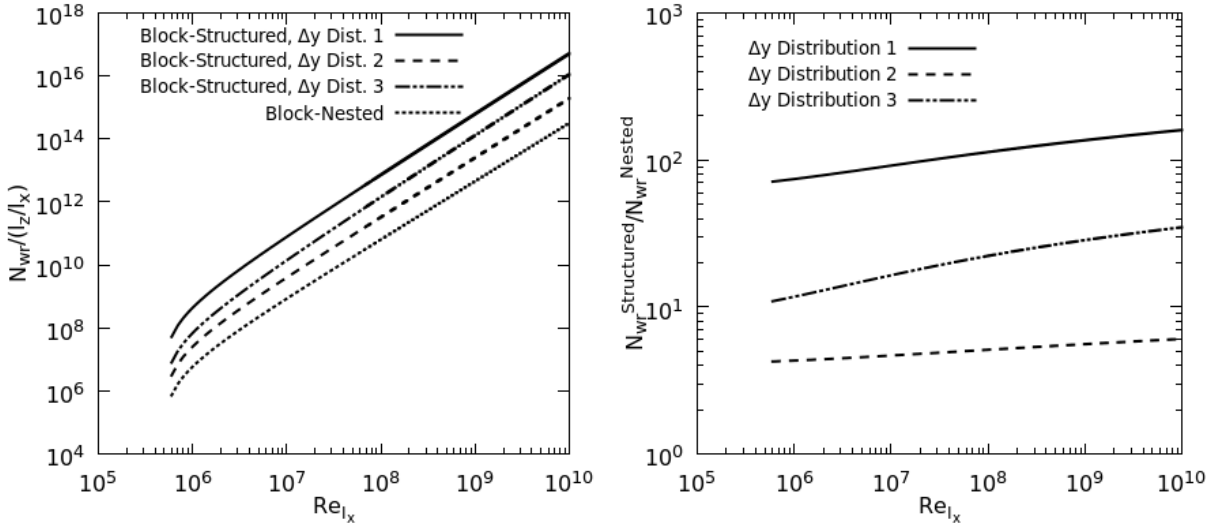

Figure 5: Variation of (left) $\mathrm{N_{wr}}/(l_z/l_x)$ estimated for the block-nested and -structured grids, and (right) the ratio of $\mathrm{N_{wr}^{Structured}}$ to $\mathrm{N_{wr}^{Nested}}$, with Re_{l_x} for ZPG-TBL. The graphs are plotted for $\mathrm{Re}_{x_0} = 5 \times 10^5$, $\eta_{\mathrm{in}} = 0.1125$, $\Delta y_1^+ = 1$, $n_{y_s} = 10$, M = 25. In addition, for the nested grid, $\Delta x_w^+ = 50$, $\Delta z_w^+ = 20$, and for the structured one, $a_x = \Delta x_w^+$, $a_z = \Delta z_w^+$.

Following the guidelines for constructing block-nested grids as reviewed in Section 2, the number of grid points required for WR-LES of domain $l_x \times \delta \times l_z$ is estimated to be,

$$\mathrm{N_{wr}} \approx \frac{n_{y_s}}{\Delta x_w^+ \Delta z_w^+} \left(\frac{l_x}{\delta}\right) \left(\frac{l_z}{\delta}\right) \frac{r_x r_z}{r_x r_z - 1} \mathrm{Re}_\tau^2 \,.$$

On the other hand, for the block-structured grid with Δy obtained by the strategies explained in Section 3.1, following estimations are derived,

$$\begin{aligned}
\mathrm{N}_{wr,1} &= \frac{1}{a_x a_z \eta_{\mathrm{in}}} \left(\frac{l_x}{\delta}\right) \left(\frac{l_z}{\delta}\right) \mathrm{Re}_\tau^2 \left[\ln \mathrm{Re}_\tau + \chi_1\right] , \\
\mathrm{N}_{wr,2} &= \frac{1}{a_x a_z \chi_3} \left(\frac{l_x}{\delta}\right) \left(\frac{l_z}{\delta}\right) \mathrm{Re}_\tau^2 \left[\ln(1+\chi_5 \mathrm{Re}_\tau) + \chi_3 \mathrm{M}(1-\eta_{\mathrm{in}})\right] , \\
\mathrm{N}_{wr,3} &= \frac{1}{a_x a_z \chi_6} \left(\frac{l_x}{\delta}\right) \left(\frac{l_z}{\delta}\right) \mathrm{Re}_\tau^2 \ln(1+\frac{\chi_6}{\Delta y_1^+} \mathrm{Re}_\tau) .
\end{aligned}$$

In these expressions, the constant grid sizes in streamwise and spanwise directions, where the flow is statistically homogeneous, are obtained from (8), which can also be written as $\Delta x = a_x \delta / \mathrm{Re}_\tau$ and $\Delta z = a_z \delta / \mathrm{Re}_\tau$ to reflect the fact that for fixed parameters a_x and a_z, flows with higher Re-number demand higher grid resolutions in x and z directions.

As shown in Fig. 6, at a specific Re-number, $\mathrm{N}_{wr} a_x a_z$ per $(l_x/\delta)(l_z/\delta)$ for the block-structured grids constructed by Δy distributions of Section 3.1, is higher than that of the equivalent block-nested grid. However, reduction in the number of grid points achieved by the block-nested strategy is less than what observed for the ZPG-TBL. In particular, the ratio of the N_{wr} of the block-structured grid to the N_{wr} of the equivalent block-nested grid can be up to $\mathcal{O}(10)$, for a fully-developed channel flow at high Re_τ.

To estimate N_{wr} for constructing block-structured grid for practical simulation of the channel flow at a specific Re_τ with known computational domain sizes (l_x/δ) and (l_z/δ), the value of parameters a_x and a_z must be appropriately chosen. In those practical simulations where estimations for the target values of Δx^+ and Δz^+ can be made a-priori, e.g. by comparing to the direct numerical simulation (DNS) data, one can simply choose $a_x = \Delta x^+$ and $a_z = \Delta z^+$. However, in accordance with the analysis performed by Chapman [2], values $\Delta x_w^+ \approx 100$ and $\Delta z_w^+ \approx 20$ can be particularly chosen for the whole domain. As mentioned earlier, more recent studies, e.g. [8, 9], have reported different appropriate values for Δx and Δz in practical simulations of channel flow. It is also noteworthy that based on another strategy that allows Δz to vary, Addad et al. [1] by analysing the streamwise and spanwise energy spectra of DNS data, reported Δx_w^+ to be approximately equal to 35 to 55. Furthermore, variable Δz^+ ranging from 15 at the wall to 45 near the center of the channel, was found to be appropriate.

4 Summary and Concluding Remarks

Estimates for the number of grid points required for constructing block-structured grids for wall-resolving LES were derived and compared to those of the block-nested grids. The main difference between the block-structured grid and the nested one is that in the former, in addition to the wall-normal resolution near the wall, the grid resolutions in the other directions proportion with the flow viscous length scale. To derive estimates for the grid resolution requirements for the block-structured grids, three functions were introduced for distributing the points in the wall-normal direction y. The main consideration in constructing these functions is that, the first off-wall grid spacing, Δy_1, relies on the appropriate choice for Δy_1^+, and the target Re-number, reflecting one of the main requirements of WR-LES that is resolving the structures of the order of the viscous length scale near the wall. This is followed by the distribution of the other points across the boundary layer bringing into account different characteristic length scales in different regions of the turbulent boundary layers.

The analyses show that, for ZPG-TBL over a flat-plate of length $(l_x - x_0)$ with $c_\mathrm{f} \sim \mathrm{Re}_x^{-\beta_f}$, at high Re-numbers, the required number of points for the block-structured grids is proportional to

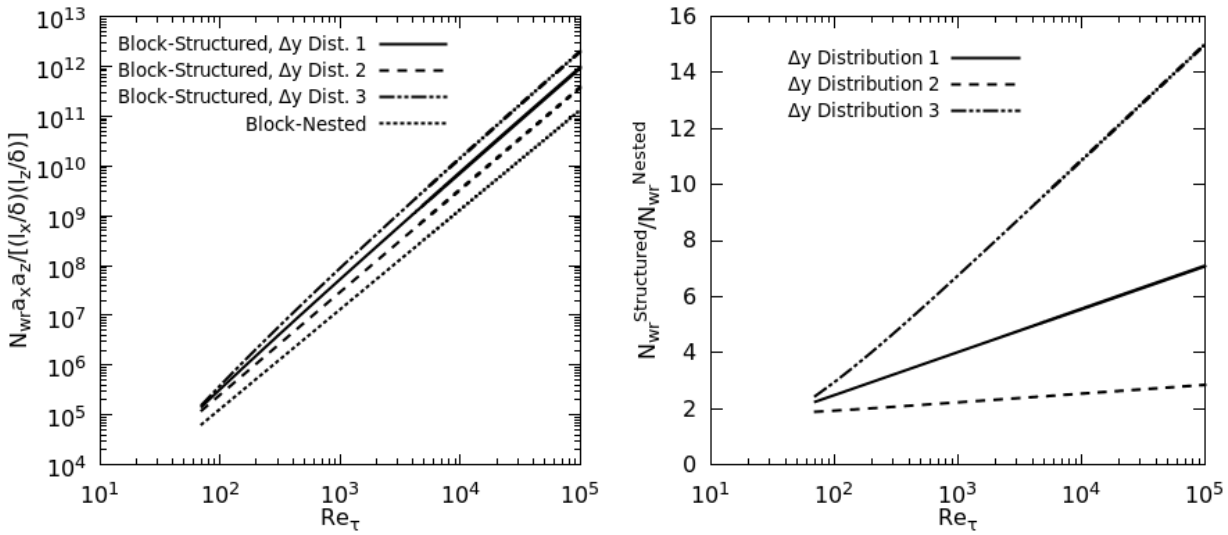

Figure 6: Variation of (left) $\mathrm{N_{wr}}a_xa_z/\left[(l_x/\delta)(l_z/\delta)\right]$ estimated for the block-nested and -structured grids, and (right) the ratio of $\mathrm{N_{wr}^{structured}}$ to $\mathrm{N_{wr}^{nested}}$, with Re_τ for fully-developed channel flow. To compare the block-nested and -structured strategies, a_x and a_z are taken to be equal to Δx_w^+ and Δz_w^+, respectively.

$\mathrm{Re}_{l_x}^{(2-\beta_f)} \ln \mathrm{Re}_{l_x}$, while for the equivalent nested strategy this proportionality relaxes to $\mathrm{Re}_{l_x}^{(2-\beta_f)}$, [2, 3]. At finite Re-numbers, comparisons reveal that depending on the specific function used for Δy, the block-structured grid requires approximately a few to $\mathcal{O}(10^2)$ times more points than the equivalent nested one, see Fig. 5. This may be an important issue to be considered when predictions for the computational cost of the simulations of the turbulent flows involving boundary layers are made.

It is also noteworthy that for fully-developed turbulent channel flow, where the block-structured grids are more convenient for practical CFD simulations, the estimates show that the ratio of the number of points of the block-structured grids to that of the block-nested ones is less than what observed for the ZPG-TBL. However, this ratio varies more significantly from one type of Δy-distribution to another one, specifically at high Re_τ. If the suggested Δy-distributions along with proper choices for Δx^+ and Δz^+ can provide acceptable results for WR-LES of channel flow, then, less improvement in computational costs is gained by employing nested grids which are relatively more difficult to handle, taking into account limitations of industrial CFD software.

To refine the estimates of the number of grid points required for WR-LES, it is necessary to thoroughly address the dependency of $\mathrm{N_{wr}}$ on different parameters such as those in the Δy-distribution functions, besides, a_x and a_z, through systematic simulations.

Acknowledgement

The computations in Appendix A.2 were performed on resources provided by the Swedish National Infrastructure for Computing (SNIC) at PDC Centre for High Performance Computing (PDC-HPC).

References

[1] Y. Addad, U. Gaitonde, D. Laurence, and S. Rolfo. Optimal unstructured meshing for large eddy simulations. In J. Meyers, B. J. Geurts, and P. Sagaut, editors, *Quality and Reliability of Large Eddy Simulations*, pages 93–103. Springer Netherlands, Dordrecht, 2008.

[2] D. R. Chapman. Computational aerodynamics development and outlook. *AIAA journal*, 17(12):1293–1313, 1979.

[3] H. Choi and P. Moin. Grid-point requirements for large eddy simulation: Chapman's estimates revisited. *Physics of Fluids*, 24(1):011702, 2012.

[4] J. Jiménez. Near-wall turbulence. *Physics of Fluids*, 25(10):101302, 2013.

[5] A. G. Kravchenko, P. Moin, and R. D. Moser. Zonal embedded grids for numerical simulations of wall-bounded turbulent flows. *J. Comput. Phys.*, 127:412423, 1996.

[6] M. Lee and R. D. Moser. Direct numerical simulation of turbulent channel flow up to $Re_\tau = 5200$. *J. Fluid Mech.*, 774:395–415, 2015.

[7] M. Liefvendahl, C. Fureby, and O. J. Boelens. Grid requirements for LES of ship hydrodynamics in model and full scale. In *31th Symposium on Naval Hydrodynamics*, Monterey, CA, June 2016.

[8] J. Meyers and P. Sagaut. Is plane-channel flow a friendly case for the testing of large-eddy simulation subgrid-scale models? *Physics of Fluids*, 19(4):048105, 2007.

[9] T. Mukha. *Inflow Generation for Scale-Resolving Simulations of Turbulent Boundary Layers*. Licentiate thesis, Department of Information Technology, Uppsala University, Sept. 2016.

[10] R. Örlü, J. H. M. Fransson, and P. H. Alfredsson. On near wall measurements of wall bounded flows-the necessity of an accurate determination of the wall position. *Progress in Aerospace Sciences*, 46:353–387, 2010.

[11] J. M. Österlund and A. Johansson. A note on the overlap region in turbulent boundary layers. *Phys. Fluids*, 12(1):1–4, 2000.

[12] S. B. Pope. *Turbulent Flows*. Cambridge University Press, 10th printing edition, 2000.

[13] S. Rezaeiravesh, M. Liefvendahl, and C. Fureby. On grid resolution requirements for LES of wall-bounded flows. In *VII European Congress on Computational Methods in Applied Sciences and Engineering*, Crete, Greece, June 2016.

[14] S. K. Robinson. Coherent motions in the turbulent boundary layer. *Annu. Rev. Fluid Mech.*, 23:601–639, 1991.

[15] S. K. Robinson. The kinematics of turbulent boundary layer structure. *NASA Technical Memorandum*, 103859:1–335, 1991.

[16] H. Schlichting and K. Gersten. *Boundary Layer Theory*. Springer, Berlin, 8th edition, 2000.

[17] J. Slotnick, A. Khodadoust, J. Alonso, D. Darmofal, W. Gropp, E. Laurie, and D. Marviplis. CFD vision 2030 study: A path to revolutionaty computational aerosciences. *NASA Technical Report*, 2014-218178, 2014.

[18] P. R. Spalart, W. H. Jou, M. Strelets, and S. R. Allmaras. Comments on the feasibility of LES for wings and on a hybrid RANS/LES approach. In *Advances in DNS/LES*, volume 1, pages 4–8, 1997.

[19] R. Vinuesa, P. Schlatter, and H. M. Nagib. Role of data uncertainties in identifying the logarithmic region of turbulent boundary layers. *Exp Fluids*, 55(1751), 2014.

[20] F. M. White. *Viscous Fluid Flow*. McGraw-Hill, Singapore, 3rd edition, 2006.

[21] E. S. Zanoun, F. Durst, and H. Nagib. Evaluating the law of the wall in two-dimensional fully developed turbulent channel flows. *Phys. Fluids*, 15(10):3079–3089, 2003.

A Appendices

A.1 ZPG-TBL Correlations

There are different types of correlations to relate the boundary layer properties to different types of Re-number, e.g. see [16, 20]. In conjunction with the estimates for grid resolution requirements for ZPG-TBL, the power-law type of correlations have been found useful because of providing the possibility of evaluating the resulting integrals analytically, e.g. see [2, 3]. The correlations of this type used in the present study can be written as,

$$\begin{aligned} c_{\mathrm{f}} &= \alpha_f \mathrm{Re}_x^{-\beta_f} , \\ \mathrm{Re}_\tau &= \alpha_\tau \mathrm{Re}_x^{\beta_\tau} , \\ \delta/x &= \alpha_\delta \mathrm{Re}_x^{-\beta_\delta} , \end{aligned}$$

for which, the values of the parameters are listed in Table 1. It must be noted that from the last two correlations, the following relations for non-dimensional viscous length scale can be derived,

$$\delta_\nu \frac{U_e}{\nu} = \frac{\alpha_\delta}{\alpha_\tau} \mathrm{Re}_x^{1-(\beta_\delta+\beta_\tau)} . \tag{14}$$

Table 1: Values of the parameters in the power-law type of correlations for ZPG-TBL, taken from [13].

α_f	β_f	α_τ	β_τ	α_δ	β_δ
0.0283	0.1540	0.0145	0.7858	0.1222	0.1372

A.2 Performance of Δy Distributions for Channel Flow

The aim is to show how the block-structured grids constructed based on the Δy-distributions of Section 3.1, can be used for simulation of fully-developed channel flow. In particular, a flow with $\mathrm{Re}_\tau = 180$, for which DNS benchmark data are available, see Table 2, is simulated using the finite-volume-based solver `OpenFOAM`[3]. The WR-LES corresponding to this Re-number are carried out considering the same domain size as the DNS case, that is instead discretized by $\mathrm{N}_x = 183$ and $\mathrm{N}_z = 114$ cells in the streamwise and spanwise directions, respectively, resulting in target $\Delta x^+ = 25$ and $\Delta z^+ = 15$. Moreover, the target Δy_1^+ is planned to converge to 1.

[3] `www.openfoam.com`

Table 2: DNS settings of the the fully-developed channel flow at $\mathrm{Re}_\tau = 180$, corresponding to Lee and Moser, [6].

Re_τ	u_τ	l_x/δ	l_z/δ	N_x	N_z	N_y	Δx^+	Δz^+	Δy_1^+
182.088	6.37309×10^{-2}	8π	3π	1024	512	96	4.47	3.35	1.0545×10^{-2}

Table 3: Results of WR-LES of the fully-developed channel flow at $\mathrm{Re}_\tau = 180$, compared to the target values.

	N_y	u_τ	Δx^+	Δz^+	Δy_1^+
Target	-	6.3731×10^{-2}	25	15	1
WR-LES with Δy distribution 1	33	6.2617×10^{-2}	24.56	14.79	0.988
WR-LES with Δy distribution 2	30	6.2402×10^{-2}	24.49	14.74	1.115
WR-LES with Δy distribution 3	40	6.2286×10^{-2}	24.44	14.71	0.898

In all WR-LES cases, second-order accurate methods are used for both spatial and temporal discretizations. In addition, the time step size is taken to be fixed and equal to 10^{-4} s. After passing the initial transients, the flow statistics were computed over 110 s. To account for the subgrid-scale effects, no explicit model is employed, meaning that the numerical dissipation supposedly plays such a role.

In Table 3, the target shear velocity and the grid spacings in wall-units are compared to the corresponding values resulted from WR-LES on the grids constructed by different Δy distributions. It is clear that despite the differences in the number of grid points and the distribution function used in the wall-normal direction, the resulting u_τ by WR-LES are similar and close to that of DNS. The same performance of all grid distributions can also be seen from the first and second-order statistical moments of velocity, as respectively shown in Fig. 7 and 8. It must be emphasized that, the conclusion on having similar performances for different Δy distributions, is only valid for the current particular Re_τ and the specific selection of parameters Δy_1^+, Δx^+ and Δz^+, besides employing the described numerical schemes. In other words, drawing any general conclusion is subject to a detailed study similar to [8], in which sensitivity and dependence of various resulting quantities of LES, such as u_τ, on the grid parameters including grid spacing in different directions as well as the distribution of the points normal to the wall, are addressed.

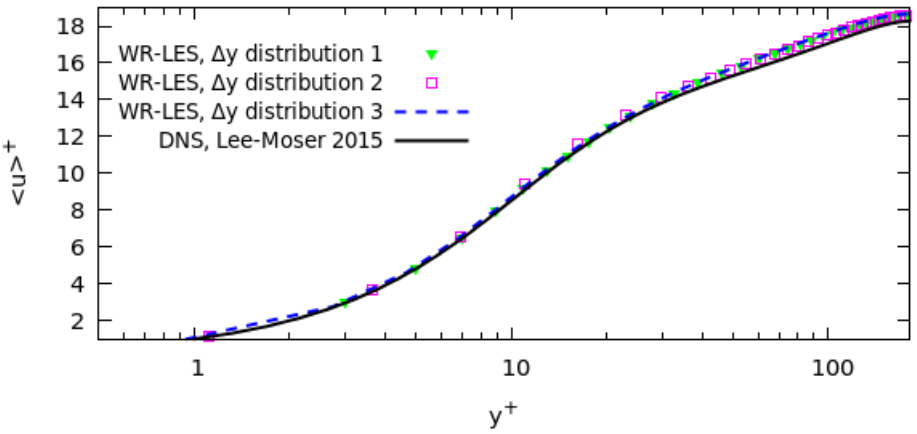

Figure 7: Inner-scaled mean velocity profiles of the fully-developed channel flow at $\mathrm{Re}_\tau = 180$. Note that $\langle \cdot \rangle$ represents averaged value over both time and homogeneous spatial directions.

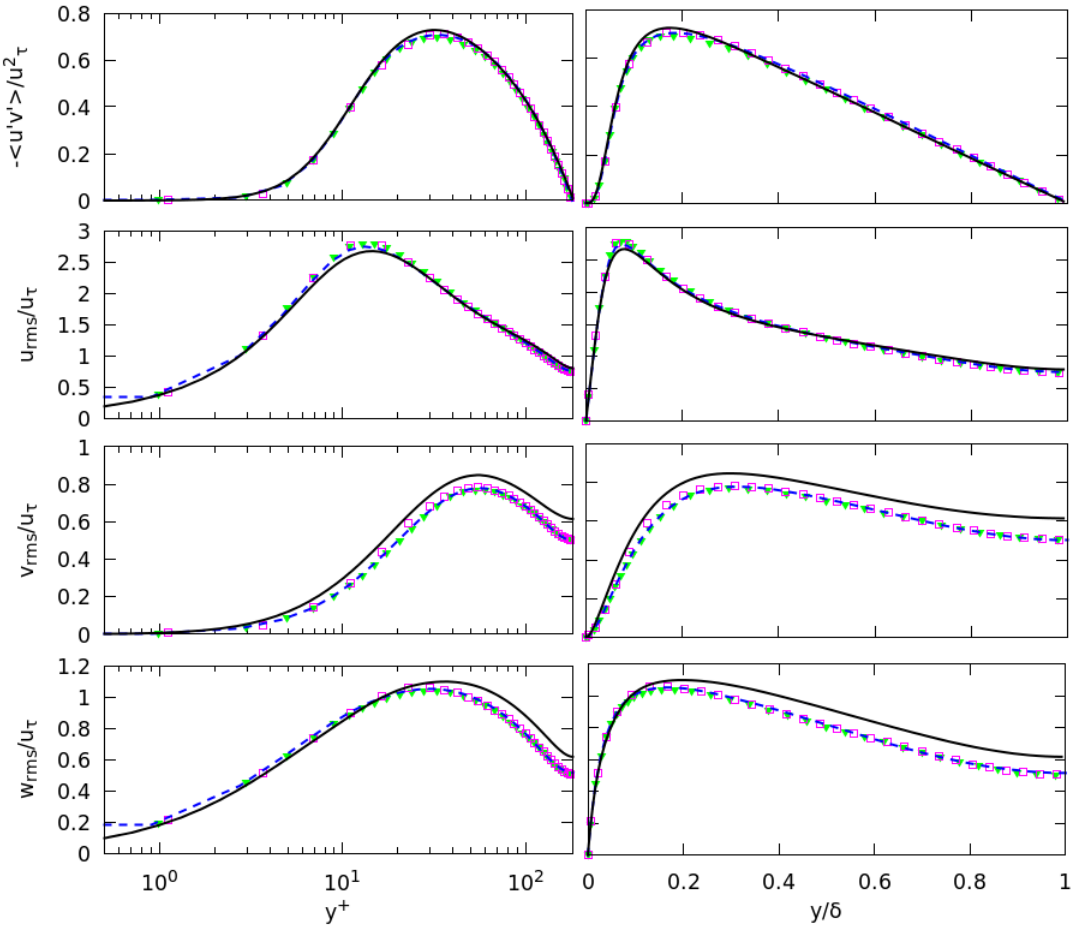

Figure 8: Profiles of Reynolds stress $\langle u'v' \rangle$ along with rms velocity components of the fully-developed channel flow at $\mathrm{Re}_\tau = 180$, normalized by shear velocity, plotted against the (left) inner-scaled, (right) outer-scaled wall-normal coordinate. For legend, see Fig. 7.